I&EC research
Industrial & Engineering Chemistry Research

pubs.acs.org/IECR

Article

Low-Viscosity Nonaqueous Sulfolane−Amine−Methanol Solvent Blend for Reversible CO_2 Capture

Jayangi D. Wagaarachchige, Zulkifli Idris, Bjørnar Arstad, Nithin B. Kummamuru, Kai A. S. Sætre, Maths Halstensen, and Klaus-J. Jens*

Cite This: *Ind. Eng. Chem. Res.* 2022, 61, 5942−5951

Read Online

ACCESS | Metrics & More | Article Recommendations | Supporting Information

ABSTRACT: In this work, the absorption−desorption performance of CO_2 in six new solvent blends of amine (diisopropylamine (DPA), 2-amino-2-methyl-1-propanol (AMP), methyldiethanolamine (MDEA), diethanolamine (DEA), diisopropanolamine (DIPA), and ethanolamine (MEA)), sulfolane, and methanol has been monitored using ATR-FTIR spectroscopy. Additionally, NMR-based species confirmation and solvent viscosity analysis were done for DPA solvent samples. The identified CO_2 capture products are monomethyl carbonate (MMC), carbamate, carbonate, and bicarbonate anions in different ratios. The DPA solvent formed MMC entirely with 0.88 mol_{CO2}/mol_{amine} capture capacity, 0.48 mol_{CO2}/mol_{amine} cyclic capacity, and 3.28 mPa·s CO_2-loaded solvent viscosity. MEA, DEA, DIPA, and MDEA were shown to produce a low or a negligible amount of MMC while AMP occupied an intermediate position.

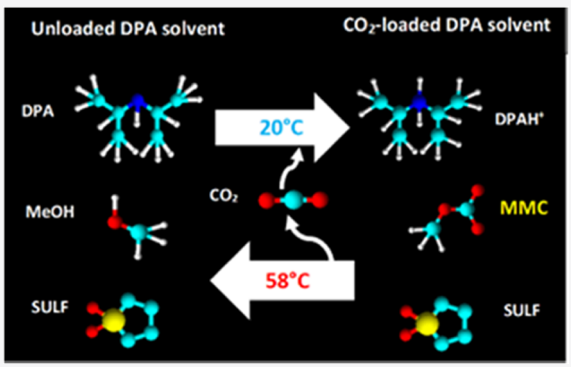

1. INTRODUCTION

Mitigation of global warming and its potential adverse effects is the greatest environmental challenge associated with the rapid increase of greenhouse gas (GHG) emissions. Anthropogenic CO_2 emissions from fossil fuel burning and other activity account for about 78% of the total GHG emissions in the last four decades.[1] Efforts from governments and industries around the world are needed to reduce greenhouse gas emissions. A major portion of the world's net CO_2 discharge originates from fossil fuel combustion in industrial processes and power generation. Postcombustion CO_2 capture (PCCC) is seen as a viable pivotal attempt to reduce global CO_2 emissions from fossil fuel combustion. The benchmark CO_2 capture technology is the gas−liquid absorption−desorption process using an aqueous 30 wt % monoethanolamine (MEA) solution. The first-generation MEA CO_2 capture solvent is known for its high reactivity and low cost.[2−4] However, the major challenge is still the high energy penalty for solvent regeneration, which is estimated to be around 4 GJ per ton of CO_2 capture.[5] Furthermore, MEA is corrosive and is shown to deteriorate pipelines and column walls[6,7] with high solvent losses due to oxidative and thermal degradations.[8]

Much research has been focused on finding CO_2 capture solvents with a lower energy penalty. Second-generation aqueous CO_2 capture solvents such as piperazine and piperazine derivatives were found to reduce operational energy expenditure by providing higher capture capacity and lowering the regeneration energy.[9,10] Other examples of these second-generation solvents include proprietary Mitsubishi's KS-1 and Fluor's advanced Econamine.[9,11] However, there is still a need for new solvent chemistries that reduce cost, e.g., mitigating energy needs.[12]

K_2Sol is a third-generation proprietary water-lean solvent system, which demonstrated reduced solvent regeneration energy of around 35% in comparison to MEA.[13] Water-lean solvents are summarized in a recent review in terms of fundamentals, uncertainties, and opportunities.[11] In these systems, typically, the solvent water portion is substituted by organics, often alcohols.[8,11,14,15] In comparison to aqueous solvents, this modifies solvent physical properties and the chemical CO_2 binding mechanism providing novel solvent chemistry but also requiring process technology adaption for potential application.

This study introduces nonaqueous sulfolane-based solvents for carbon capture that can regenerate at low temperatures. Sulfolane, methanol, and amine are the three components of these solvents. Sulfolane (SULF) is a well-known industrial chemical that can be used as a low-volatile organic diluent. It is a polar aprotic solvent with a strong affinity for acid gases.[16,17]

Received: December 22, 2021
Revised: April 13, 2022
Accepted: April 14, 2022
Published: April 25, 2022

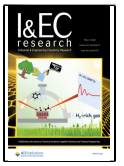

Table 1. Information of Chemicals Used in This Work[a,b,c,d,e]

Chemical name	CAS number	Chemical structure	Purity [a] (%)	pKa	Supplier
2-amino-2-methyl-1-propanol (AMP)	124-68-5	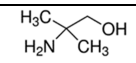	≥0.99	9.73[b]	Sigma-Aldrich
diisopropylamine (DPA)	108-18-9	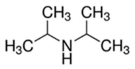	≥0.99	11[c]	Sigma-Aldrich
methyldiethanolamine (MDEA),	105-59-9	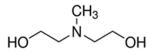	≥0.99	8.56[d]	Sigma-Aldrich
diisopropanolamine (DIPA)	110-97-4	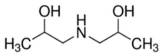	≥0.98	8.88[d]	Sigma-Aldrich
diethanolamine (DEA)	111-42-2	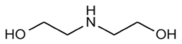	≥0.99	8.88[d]	Sigma-Aldrich
ethanolamine (MEA)	141-43-5	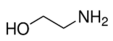	≥0.99	9.45[c]	Sigma-Aldrich
Sulfolane (SULF)	126-33-0		≥0.99	n.a.	Sigma-Aldrich
Methanol (MeOH)	67-56-1		≥0.99	n.a.	VWR
Carbon dioxide (CO_2)	124-38-9	O=C=O	0.99999	n.a.	AGA Norge AS

[a]As given by the supplier. [b]Kim et al.[30] [c]Zeng et al.[31] [d]Kim et al.[32] [e]n.a.: not applicable.

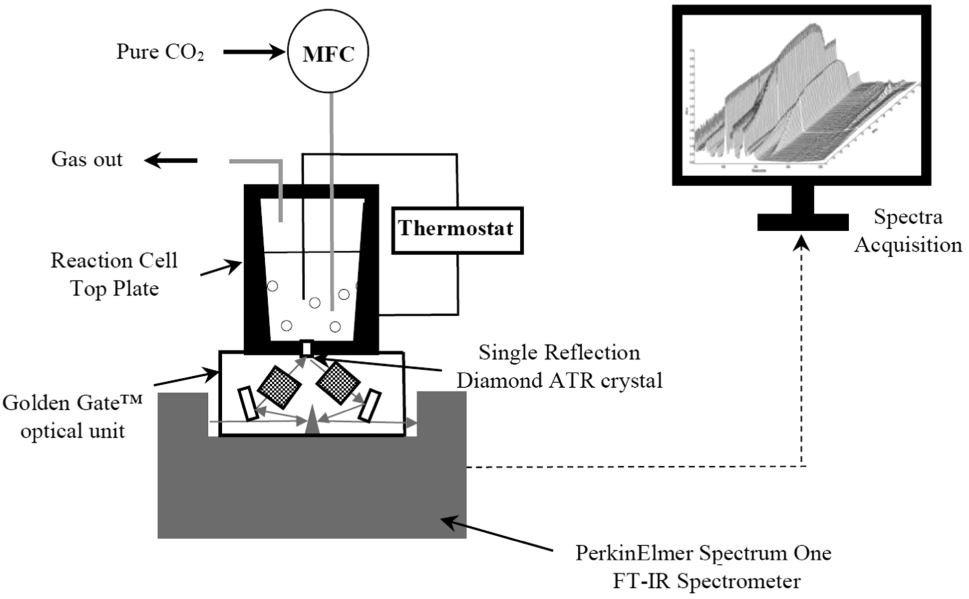

Figure 1. Schematic diagram for ATR-FTIR in situ monitoring.

Sulfolane enhances CO_2 absorption rate and solubility during the chemical absorption without participating in the chemical reaction.[18] In a recent article by Zou et al.,[19] it was shown that the addition of sulfolane enables higher absorption and desorption rates and higher cyclic capacity in CO_2 capture in comparison to the aqueous MEA. A study on the sulfolane-based semiaqueous piperazine (PZ) system concluded that addition of sulfolane increased the equilibrium constant at medium CO_2 loadings and slightly increased the CO_2 cyclic capacity.[20] Lidong and co-workers suggested that addition of sulfolane to make a semiaqueous system of diethylenetriamine (DETA) resulted in a higher CO_2 removal rate and energy-saving than the respective aqueous solvent.[21,22] However, there is also a claim that sulfolane affects corrosion in the presence of water, oxygen, or oxidizing agents.[23]

The second component in our reported solvents is methanol. It has the ability to reduce the heat capacity of solvent blends.[24] In addition, it was investigated as a component for hybrid solvents to reduce regeneration cost due to its low boiling point, low viscosity, and lower corrosivity than water.[25,26] Sulfolane and methanol are commercially available organic chemicals that are used in Sulfinol[16,27] and Aminol[28] processes, respectively. The third solvent component is commercially available amines MEA, 2-amino-2-methyl-1-propanol (AMP), diisopropylamine (DPA), methyldiethanol-

https://doi.org/10.1021/acs.iecr.1c04946
Ind. Eng. Chem. Res. 2022, 61, 5942−5951

amine (MDEA), diethanolamine (DEA), and diisopropanolamine (DIPA).

The most promising solvent blend was characterized using nuclear magnetic resonance (NMR) spectroscopy to confirm monomethyl carbonate (MMC) formation. MMC is the simplest species of monoalkyl carbonic acid ester compounds that can easily be decomposed at a mild temperature.[29] In addition, viscosity measurements were also performed on the most promising solvent type.

2. MATERIALS AND METHODS

2.1. Solvent/Sample Preparation. Details of chemicals used in this study are listed in Table 1. These chemicals were used as received without further purification.

As part of our interest in sulfolane-based nonaqueous CO_2 capture solvents, the reported solvent composition was found by serendipity. The DPA solvent was prepared by mixing 30% DPA, 35% methanol, and 35% sulfolane, resulting in a molar ratio of 1.000, 3.6846, and 0.9824 for DPA, methanol, and sulfolane, respectively. All other solvent amine (AMP, MDEA, DIPA, MEA, and DEA) mixtures are prepared in a manner that achieves the same molar ratios. All of the samples contain 14.8 mmol of amine, 54.6 mmol of methanol, and 14.5 mmol of sulfolane. A PB-303S analytical weighing balance from Mettler Toledo with an accuracy of ±0.01 g was used to weigh the required amount of chemicals.

2.2. Solvent Screening with In Situ ATR-FTIR Analysis. The schematic diagram of the ATR-FTIR spectroscopy setup is shown in Figure 1.

To evaluate the effectiveness of the solvents, CO_2 absorption and desorption tests were performed in a reaction cell top plate (P/N GS10507) connected to a Golden Gate single reflection diamond ATR system (GS10500 Series). The reaction cell is a stainless steel double-jacketed conical-cylindrical chamber with a stainless steel top plate, a type-K thermocouple, and stainless steel tubing for the gas inlet and outlet. The empty cell was first flushed with high-purity nitrogen gas (N_2) for several minutes, and then an ATR-FTIR background scan was collected. Prior to the absorption experiment, a known amount of solvent was placed inside the reaction cell according to Table 2, and the top plate was tightened properly. Absorption and desorption experiments were conducted at two different temperatures of 20 and 58 °C continuously for around 2 h. In situ reaction monitoring was performed using a PerkinElmer Spectrum One FTIR spectrometer. IR spectra were recorded every minute using PerkinElmer's TimeBase software. Each IR spectrum was an average of 16 scans in the wavenumber range of 400−4000 cm^{-1} at a resolution of 4.0 cm^{-1}. Before CO_2 was introduced into the reaction cell, several ATR-FTIR scans of the fresh solvent were taken. During these scans, only peaks corresponding to the amine, MeOH, and SULF blend were observed. CO_2 gas was introduced into the reaction cell at a flow rate of 0.02 L/min using a mass flow controller (MFC) from Sierra Instruments. After reaching the maximum height of increasing CO2-related peaks, the CO_2 flow was set to zero and the temperature of the ATR-FTIR reaction cell was increased to 58 °C. A typical desorption experiment lasted around 40 min until the minimum decreasing peak intensity was reached. For quantification of the liquid sample CO_2-loading at the end of the experiments, the $BaCl_2$ titration method was used.[33]

Table 2. Solvent Sample Weights Used in ATR-FTIR In Situ Monitoring

solvent amine type	mass of sample (g)
DPA	5.00
AMP	4.82
MDEA	5.27
DIPA	5.47
MEA	4.40
DEA	5.05

2.3. ^{13}C and ^{1}H NMR Spectroscopy Analysis. ^{13}C and ^{1}H NMR experiments were performed for the unloaded and CO_2-loaded DPA solvent samples. The NMR measurements were performed for qualitative molecular structure identification and confirmation of FTIR band assignment. Analysis was conducted using a Bruker Avance III 400 MHz spectrometer with a BBFO Plus double-resonance probe head at 298 K. After acquisition, the spectra were processed using MestreNova software v 10.0.2. The ^{13}C NMR spectra were processed by proper signal phasing and baseline correction. A line broadening factor of 1.5 Hz was applied to enhance the signal-to-noise ratio.

2.4. Viscosity Determination. For viscosity analysis of the DPA solvent, predetermined CO_2-loaded samples were prepared by bubbling pure CO_2 gas into an unloaded solvent. The actual CO_2 content was confirmed by the $BaCl_2$ titration method.[33] Regeneration of the CO_2-loaded solvents was performed at 60 °C in a laboratory-scale CO_2 desorption apparatus as shown in Figure 2. The solvent was heated at 60 °C with stirring for 2 h to ensure complete regeneration.

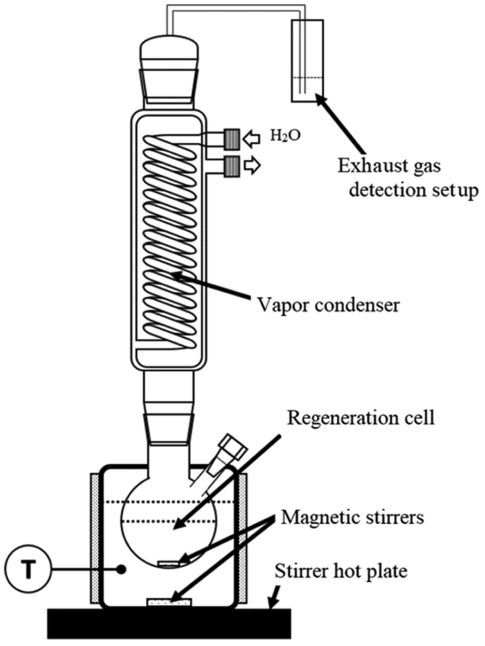

Figure 2. Schematic diagram of the laboratory-scale CO_2 desorption apparatus.

An Anton Paar Physica MCR 101 rheometer with a doubled-gap pressure cell XL was used to measure the dynamic viscosity of the unloaded, CO_2-loaded, and regenerated DPA solvent. The measurements in this work were taken at 40 °C using the procedure described in our previous publication.[34] The rheometer used for the viscosity

https://doi.org/10.1021/acs.iecr.1c04946
Ind. Eng. Chem. Res. 2022, 61, 5942−5951

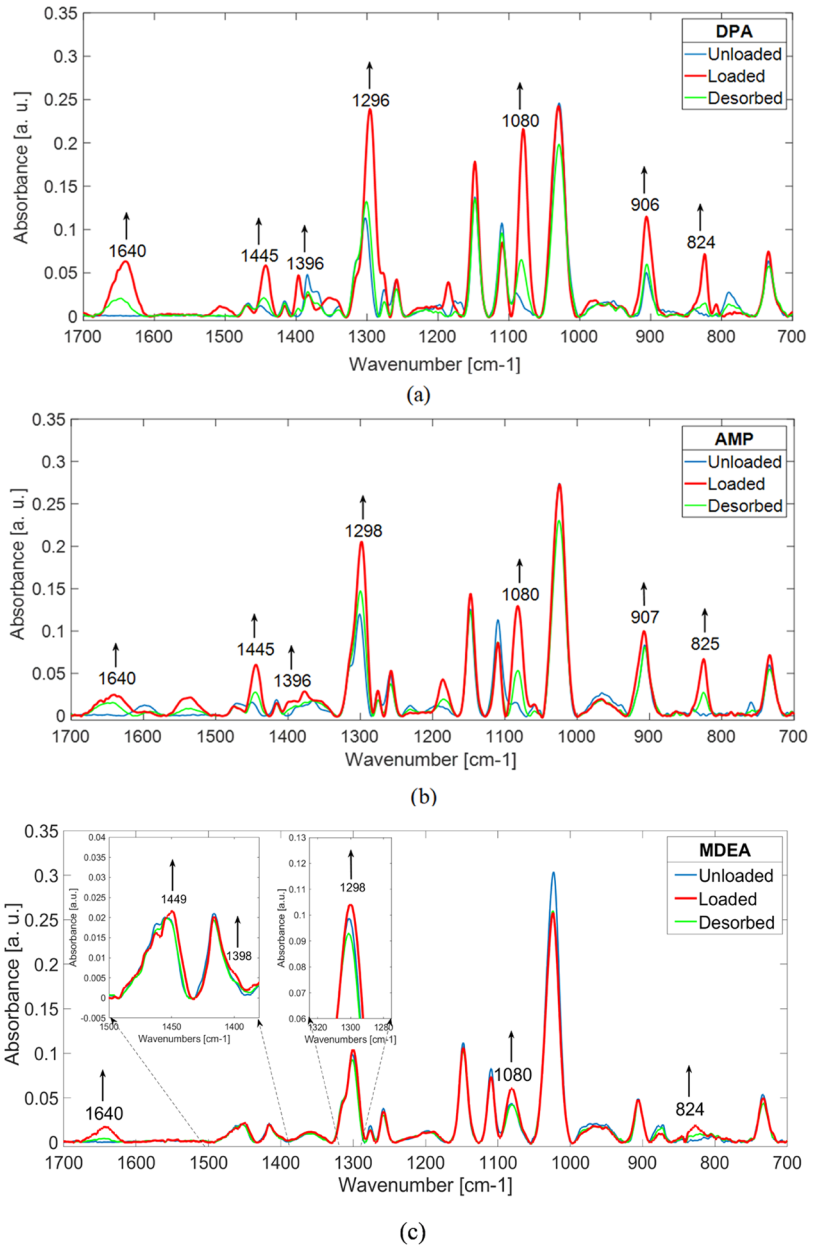

Figure 3. Baseline-corrected ATR-FTIR spectra of unloaded (blue line), CO_2-loaded (red line), and desorbed (green line) DPA (a)-, AMP (b)-, and MDEA (c)-based solvents.

measurements has a standard uncertainty for temperature and torque of 0.03 K and 0.0002 Nm, respectively.

3. RESULTS AND DISCUSSION

The results of the solvent screening experiments are discussed in this section. MMC and carbamate formation during CO_2 absorption are discussed based on FTIR vibrational band assignments. Confirmation of MMC formation for the best-performing solvent (DPA) is discussed using ^{13}C and ^{1}H NMR spectroscopy results. This is then followed by a discussion of solvent viscosity.

3.1. ATR-FTIR In Situ Monitoring: CO_2 Absorption and Desorption. As explained in Section 2.2, CO_2 absorption and desorption experiments of six sulfolane-based solvents were monitored using ATR-FTIR.

To identify the reaction products, the IR spectra were baseline-corrected and the vibrational modes of possible CO_2 capture products were assigned according to the corresponding wavenumbers. The baseline-corrected spectra of unloaded, CO_2-loaded, and regenerated DPA-, AMP-, and MDEA-based solvents are shown in Figure 3a–c, respectively.

New species are formed when CO_2 reacts with the solvent, and these are indicated by formation of new FTIR peaks. In Figure 3a, new peaks at 1640, 1443, 1396, 1298, 1080, 906, and 824 cm^{-1} were observed for the DPA-based solvent. These peaks decreased during desorption, suggesting a mild temperature regeneration ability of the DPA-based solvent. Table 3 summarizes these peaks and their respective IR vibrational modes. Earlier work by Behrendt and co-workers show these new peaks observed in the DPA solvent to be indicative of MMC formation.[35] Furthermore, IR peaks at 1636 and 1290 cm^{-1} assigned to an alkylcarbonate species were also observed by Yang et al.[8] in the CO_2-loaded nonaqueous solvent of 2-piperidineethanol (2-PE) and ethylene glycol (EG). IR

https://doi.org/10.1021/acs.iecr.1c04946
Ind. Eng. Chem. Res. 2022, 61, 5942−5951

Table 3. FTIR Peak Identification of DPA-, AMP-, and MDEA-Based Solvents[a]

characteristic IR vibrational bands, ν_{max} (cm^{-1})			
DPA	AMP	MDEA	IR peak assignment
1640	1640	1640	C═O stretching vibration[8,35,38]
1445	1445	1449	CH_3 asymmetric deformation[35,38]
1396	1396	1398	CH_3 symmetric deformation[35,38]
1296	1298	1298	O−C−O asymmetric stretching vibration[8,35,38]
1080	1082	1080	O−C−O symmetric stretching vibration[35,38]
906	907	n.o.	CH_3−O stretching[35,38]
824	824	824	CO_3 deformation[35,38]

[a]n. o.: not observed.

carbamate peaks are normally observed[8,36,37] in the wavenumber range of 1550−1450 cm^{-1}. Interestingly, no carbamate peaks were visible, indicating no carbamate end-product formation for the CO_2-loaded solvent. IR peaks of the DPA-, AMP-, and MDEA-based solvents are assigned to the respective IR vibrational modes in Table 3. Interestingly, MDEA exhibits only a negligible amount of MMC.

Figure 4 shows the baseline-corrected unloaded, CO_2-loaded, and regenerated spectra of the MEA sulfolane solvent. The peak development pattern during CO_2 absorption was slightly different from those of the aforementioned DPA and AMP-based solvents. The newly increased peaks included MMC vibrational wavenumbers, but the maximum peak height was considerably lower than those of DPA- and AMP-based solvents. During mild temperature desorption, these peaks were reduced. Three additional peaks at 1574, 1486, and 1382 cm^{-1} were also observed during CO_2 absorption. These peaks represent the asymmetric and symmetric stretching bands of MEA-carbamate[8,36,37,39] and C−O stretching bands of the carbonate[37,39] (CO_3^{2-}) anion. Similar behavior with strong carbamate formation with few alkylcarbonate species was observed by Chen and co-workers for the MEA/EG non-aqueous solvent.[8] The former peaks did not change during desorption, suggesting that a higher temperature was required for a complete regeneration for the MEA-based solvent. It is well known that carbamate requires a high temperature for regeneration. Similar behavior as that of the MEA-based solvent was seen for the DEA- and DIPA-based solvents; reaction with CO_2 for these solvents produced a mixture of carbamate and MMC species, and the carbamate needed a higher temperature for complete regeneration. FTIR spectra for DEA- and DIPA-based solvents are provided in Figure S1.

In FTIR spectroscopy, the chemical species concentration is directly proportional to the corresponding peak area or, as an approximation, the peak height. The distinctive MMC peak at 1080 cm^{-1} is used for qualitative comparison of MMC formation between these solvents. Based on Figure 5, it can be seen that DPA produces most MMC, followed by AMP, MEA, DEA, and DIPA. MDEA is not included in this and other comparisons below due to its negligible formation of MMC.

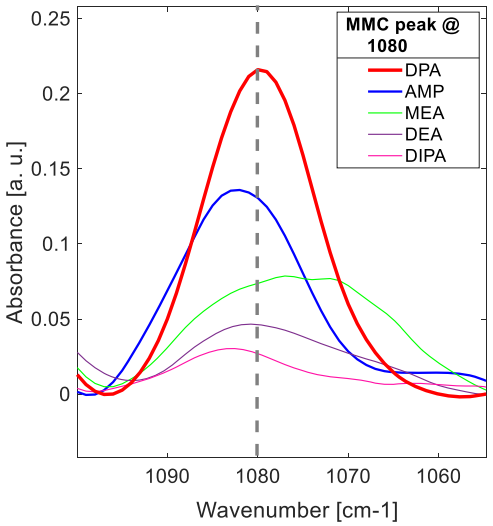

Figure 5. FTIR-based comparison of MMC formation of five solvents tested in this work.

CO_2 cyclic capacity, the difference between rich loading and lean loading, is an important solvent feature.[40] This property is of special interest for process design in terms of solvent flow rates, size of the absorber and stripper, etc. In this work, results from continuous CO_2 absorption and desorption experiments on five solvents were used to evaluate their CO_2 capture and cyclic capacities. A typical example of time-based ATR-FTIR spectra obtained for the DPA solvent is shown in Figure 6. Formation of peaks corresponding to MMC can be seen

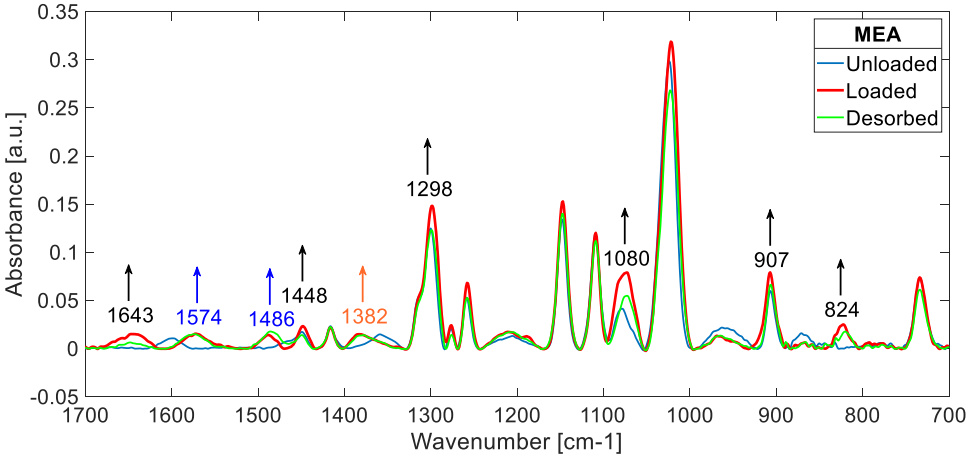

Figure 4. Baseline-corrected ATR-FTIR spectra of unloaded (blue line), CO_2-loaded (red line), and desorbed (green line) MEA solvent.

https://doi.org/10.1021/acs.iecr.1c04946
Ind. Eng. Chem. Res. 2022, 61, 5942−5951

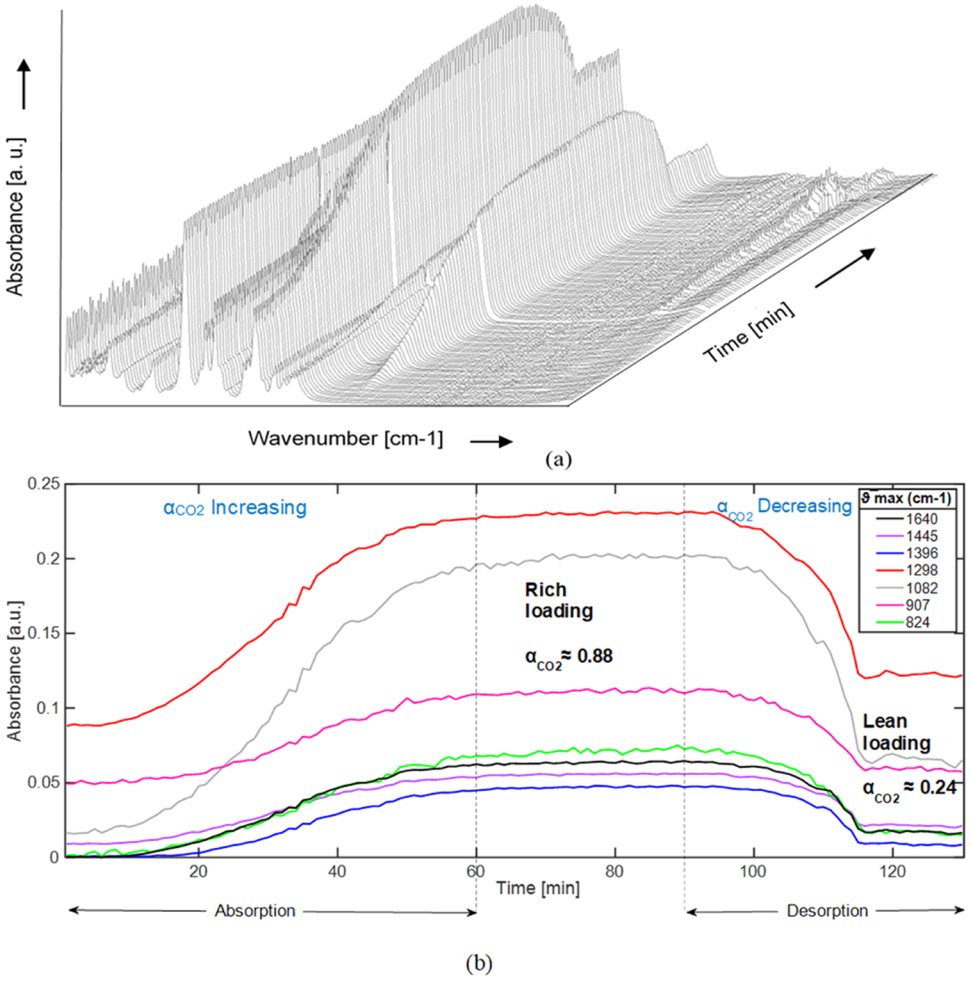

Figure 6. CO_2 absorption−desorption cycle of the DPA solvent over time. ATR-FTIR scans (a) and MMC IR vibrational band variation (b).

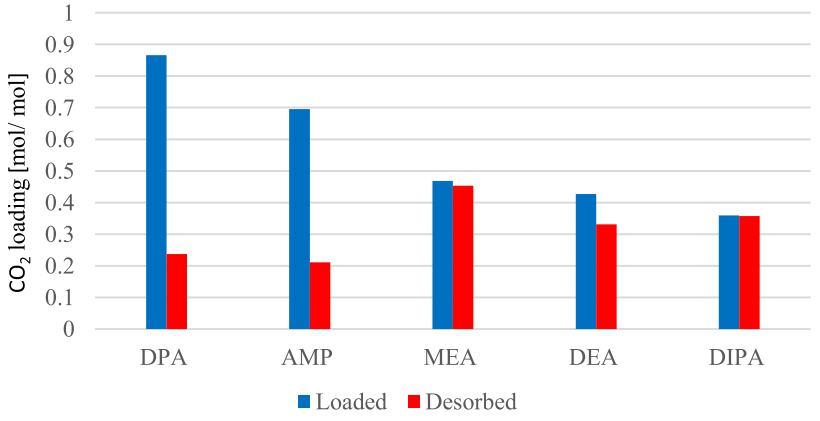

Figure 7. CO_2-rich and -lean loading of five investigated solvents.

clearly; these peaks decreased during the desorption step. At the end of absorption and desorption experiments, liquid samples were collected and titrated using the $BaCl_2$ method to determine the CO_2 loadings (α). The results obtained are depicted in the bar chart as shown in Figure 7. At an absorption temperature of 20 °C, the DPA solvent has the highest CO_2 capture capacity with α of 0.88 mol_{CO2}/mol_{amine}, followed by the AMP solvent with an α of 0.695 mol_{CO2}/mol_{amine}. On the other hand, MEA, DEA, and DIPA solvents showed lower α of 0.467, 0.426, and 0.358 mol_{CO2}/mol_{amine}, respectively. Overall, the maximum α of the DPA solvent is close to 1, which corresponds to the stoichiometry of MMC formation in the nonaqueous solvent. The low CO_2 capture capacity seen in the case of MEA, DEA, and DIPA solvents may be attributed to the reaction stoichiometry based on the carbamate formation. During desorption experiments at a temperature of 58 °C, α of the regenerated samples of DPA and AMP solvents was reduced by around 70% suggesting that the capture products are reversible at a low temperature. No noticeable change in α was observed during desorption for

https://doi.org/10.1021/acs.iecr.1c04946
Ind. Eng. Chem. Res. 2022, 61, 5942−5951

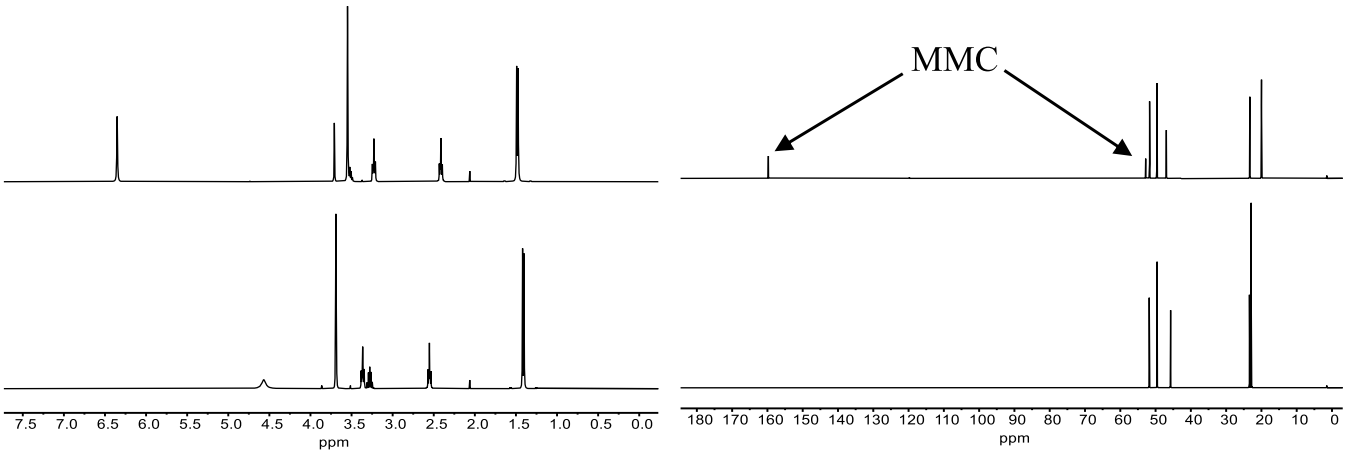

Figure 8. ^{1}H (left) and ^{13} C (right) NMR spectra of CO_2-loaded (top) and unloaded (bottom) DPA nonaqueous solvent.

MEA, DEA, and DIPA solvents, which can be attributed to the stable carbamate formation in these solvents.

Based on Figure 7, the cyclic capacity for CO_2 absorption for each of the solvents tested in this work can be calculated by subtracting the lean loading at 58 °C from the rich loading at 20 °C. The DPA solvent has the highest cyclic capacity of 0.629 mol_{CO2}/mol_{amine}. This is followed by AMP, DEA, MEA, and DIPA with cyclic capacities of 0.484, 0.096, 0.015, and 0.002 mol_{CO2}/mol_{amine}, respectively. As a comparison, aqueous 30 wt % MEA cyclic capacity is reported to reach between 0.34 and 0.1 mol_{CO2}/mol_{amine}.[14,41] Cyclic capacities of RTI's NAS solvents have been reported to be between 0.2 and 0.4 mol_{CO2}/mol_{amine}.[14] The cyclic capacity of the proposed nonaqueous solvent by Chen and co-workers was around 1 mol_{CO2}/mol_{amine}.[8] The relatively high cyclic capacity of our DPA solvent is beneficial for the design of absorption and desorption columns. Since it is superior in terms of cyclic capacity to the other tested solvent examples, it was selected for further characterization as discussed below.

3.2. NMR Results of DPA Solvent and the Mechanism of Reaction. Typical ^{13}C and ^{1}H NMR spectra of unloaded and CO_2-loaded DPA solvent are shown in Figure 8, whereas the ^{13}C and ^{1}H chemical shift values of the species are tabulated in Table 4.

Two new peaks at 53.1 and 160.1 ppm can be observed in the ^{13}C NMR spectrum of the CO_2-loaded DPA solvent, and two new peaks appeared at 6.3 and 3.4 ppm in the ^{1}H NMR spectrum. The peak at 160.1 ppm has been identified earlier as the ^{13}C NMR signal of the carbon atom of the $-OCO_2-$ moiety in the MMC group.[8,42] The resonance at 53.1 ppm corresponds to the methyl carbon of MMC derived from MeOH.[8] In the ^{1}H NMR spectrum of the CO_2-loaded solvent, the peak at 6.3 ppm is attributed to the methylcarbonate group and the peak at 3.4 ppm represents the signal of the methyl group of MMC and DPA. There was no sign of carbamate formation in the ^{1}H NMR spectra: however, carbamate has a distinctive ^{13}C NMR signal at 164 ppm[8,42−44] which was not observed either. Hence, the sample does not contain carbamate anions. Overall, the NMR results confirm that both DPA and MeOH take part in the CO_2 absorption reaction by forming MMC as the sole CO_2-containing product.

Table 4. ^{1}H and ^{13}C Chemical Shift Values of Unloaded and Loaded Samples of DPA Solvent

		chemical shift values [ppm]	
sample	species	^{1}H	^{13}C
unloaded	DPA	1.3 and 3.2	20.3 and 47.3
	methanol	3.6	49.9
	sulfolane	2.5 and 3.3	23.6 and 52.1
	exchange peak[a]	4.5	
CO_2-loaded	DPA	1.4 and 3.4	23.2 and 46.1
	methanol	3.6 (unreacted)	49.9
	sulfolane	2.3 and 3.1	23.7 and 52.0
	MMC	3.4 (methyl) and 6.3 (carbonate)	53.1 and 160.1

[a]Exchange peak denotes fast exchanging amine/protonated amine protons.

For alcohol-containing nonaqueous AMP solution, alkylcarbonate formation is suggested to occur by nucleophilic alcoholysis of the unstable AMP carbamate intermediate.[45,46] In analogy to this proposed mechanism, Figure 9 shows the proposal for the DPA solvent. Alkylcarbonate formation in the anhydrous alcoholic condition is thought not to occur through the reaction of tertiary amine and CO_2 since tertiary amines do not form carbamate species.[45]

In contrast, the reaction of CO_2 with alcohol or alcohol derivatives and tertiary amines in the neat state[47,48] or in a nonaqueous solution of primary or secondary amine[49] leads to alkylcarbonate formation. It is proposed that in the latter case, the hydroxyl group functions as a nucleophile toward CO_2; the amine stabilizes both the nucleophilic hydroxyl group and the alkylcarbonic acid ester product as shown in Figure 10.[49]

Both DPA and AMP are steric-hindered amines,[50] which should form intermediate carbamate species. Our data does not provide indications to which and what extent the two above-proposed alkylcarbonate mechanisms would apply for the amines of this work; however, concurrent operation of both mechanisms in analogy[49,53] to CO_2 absorption into aqueous alkanolamine solution seems possible for all alkanolamine solvents of this work. Elucidation of what governs the amount of formed MMC including the high reactivity of the DPA solvent requires further work.

3.3. DPA Solvent Viscosity. Solvent viscosity is a critical parameter of the CO_2 capture solvent since it affects column design. Viscous solvents cause lower CO_2 capture efficiency due to reduced mass transfer. Additionally, larger heat exchangers are needed for highly viscous solvents due to

https://doi.org/10.1021/acs.iecr.1c04946
Ind. Eng. Chem. Res. 2022, 61, 5942−5951

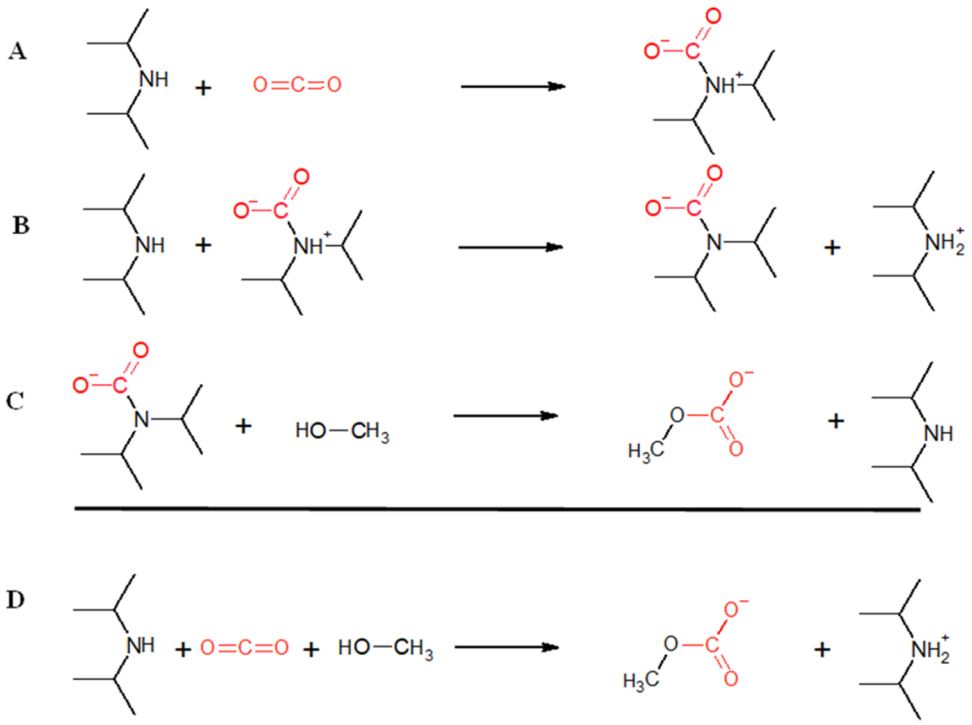

Figure 9. Possible reaction mechanism for monomethyl carbonate formation by the nucleophilic attack of methanol on intermediate DPA carbamate proposed in analogy to the literature.[45,46]

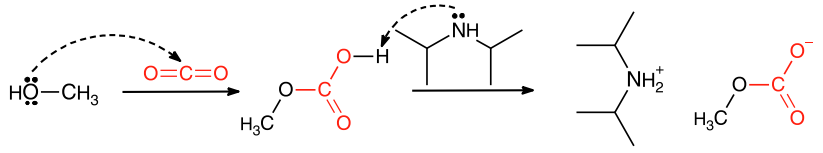

Figure 10. Possible alkylcarbonate formation through deprotonation of methylcarbonic acid proposed in analogy to the literature.[49]

their lower heat transfer, which leads to extra capital costs. One of the main concerns with nonaqueous solvent is the high viscosity of the solution upon exposure to CO_2.[11]

Viscosity results for the DPA solvent are compared to the reported viscosity of 30 wt % MEA[12] and are shown in Figure 11. At 40 °C, the viscosity of the DPA solvent only minimally increased from 1.02 mPa·s for unloaded to 3.28 mPa·s at a loading of 0.88 mol_{CO2}/mol_{amine}. This is comparable to the benchmark 30 wt % MEA solvent in which the viscosity changes from 1.7 to 2.7 mPa·s at 40 °C from lean to rich streams.[14,51] Other nonaqueous solvents tend to have high viscosity. For example, the RTI's NAS2 and Gen2 NAS both have a viscosity of 27.1 and 9.34 mPa·s upon CO_2 uptake.[14] The CO_2-binding organic solvents CO_2BOLs on the other hand show viscosities in the range of 200 mPa·s upon CO_2 absorption.[14,52] The comparable viscosity of the DPA solvent studied in this work with that of MEA is beneficial.

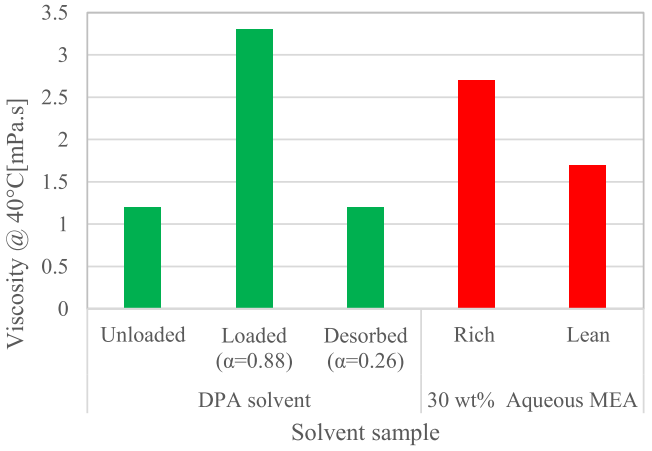

Figure 11. Viscosity comparison: DPA (green columns) solvent with 30% aqueous MEA (red columns) at 40 °C.

4. CONCLUSIONS

Six new CO_2 capture solvent blends, each composed of amine (DPA, AMP, MDEA, DEA, DIPA, MEA), sulfolane, and methanol, were prepared and screened for CO_2 absorption and desorption capability, which was monitored by ATR-FTIR spectroscopy. CO_2 was captured through formation of monomethyl carbonate (MMC) and carbamate anion. The ratio of these species toward each other was different for the various amines; DPA formed exclusively MMC, while MDEA, MEA, DEA, and DIPA did not or rarely formed it. AMP occupies an intermediate position in this group of amines. The solvent speciation is confirmed by IR literature reference and NMR analysis of the DPA solvent. MMC can be readily decomposed to amine and CO_2 at a temperature of around 60 °C. The solvent viscosity (T = 40 °C) changes from 1.02 to 3.28 mPa·s for unloaded to fully CO_2-loaded (α = 0.88) solvents. This viscosity data is comparable to that of aq. 30 wt

https://doi.org/10.1021/acs.iecr.1c04946
Ind. Eng. Chem. Res. 2022, 61, 5942−5951

% MEA solvent. Further work must consider an optimal solvent blend composition and the effect of water on solvent CO_2 capture performance.

■ ASSOCIATED CONTENT

Supporting Information

The Supporting Information is available free of charge at https://pubs.acs.org/doi/10.1021/acs.iecr.1c04946.

Baseline-corrected ATR-FTIR spectra of unloaded, CO_2-loaded, and desorbed DEA and DIPA solvents and viscosities at 40 °C of DPA (PDF)

■ AUTHOR INFORMATION

Corresponding Author

Klaus-J. Jens − *Department of Process, Energy and Environmental Technology, University of South − Eastern Norway, 3918 Porsgrunn, Norway;* orcid.org/0000-0002-9022-5603; Phone: +4735575193; Email: Klaus.J.Jens@usn.no

Authors

Jayangi D. Wagaarachchige − *Department of Electrical, IT and Cybernetics, University of South − Eastern Norway, 3918 Porsgrunn, Norway*

Zulkifli Idris − *Department of Process, Energy and Environmental Technology, University of South − Eastern Norway, 3918 Porsgrunn, Norway;* orcid.org/0000-0001-7905-9686

Bjørnar Arstad − *SINTEF Materials and Chemistry, 0314 Oslo, Norway*

Nithin B. Kummamuru − *Department of Process, Energy and Environmental Technology, University of South − Eastern Norway, 3918 Porsgrunn, Norway*

Kai A. S. Sætre − *Department of Process, Energy and Environmental Technology, University of South − Eastern Norway, 3918 Porsgrunn, Norway*

Maths Halstensen − *Department of Electrical, IT and Cybernetics, University of South − Eastern Norway, 3918 Porsgrunn, Norway*

Complete contact information is available at: https://pubs.acs.org/10.1021/acs.iecr.1c04946

Author Contributions

The manuscript was written through the contributions of all authors. All authors have given approval to the final version of the manuscript.

Funding

This work was funded by the Ministry of Education and Research of the Norwegian Government.

Notes

The authors declare no competing financial interest.

■ ABBREVIATIONS USED

ATR-FTIR	attenuated total reflectance fourier transform infrared
MMC	monomethyl carbonate
CO_2	carbon dioxide
DPA	diisopropylamine
AMP	2-amino-2-methyl-1-proponol
MEA	monoethanolamine
DEA	diethanolamine
DIPA	diisopropanolamine
MDEA	methyldiethanolamine
MAC	monoalkyl carbonate
MeOH	methanol
α	CO_2 loading
NMR	nuclear magnetic resonance
NAS	nonaqueous solvent
2-PE	2-piperidineethanol
EG	ethylene glycol

■ REFERENCES

(1) Pachauri, R. K.; Allen, M. R.; Barros, V. R.; Broome, J.; Cramer, W.; Christ, R.; Church, J. A.; Clarke, L.; Dahe, Q.; Dasgupta, P. *Climate Change 2014: Synthesis Report. Contribution of Working Groups I, II and III to the Fifth Assessment Report of the Intergovernmental Panel on Climate Change*; IPCC, 2014.

(2) Rochelle, G. T. Amine Scrubbing for CO_2 Capture. *Science* **2009**, *325*, 1652−1654.

(3) Lepaumier, H.; Picq, D.; Carrette, P.-L. New Amines for CO_2 Capture. I. Mechanisms of Amine Degradation in the Presence of CO_2. *Ind. Eng. Chem. Res.* **2009**, *48*, 9061−9067.

(4) Roberts, R. B. Process for Separating Acidic Gases. U.S. Patent US1,783,9011930.

(5) Sodiq, A.; Hadri, N. E.; Goetheer, E. L. V.; Abu-Zahra, M. R. M. Chemical reaction kinetics measurements for single and blended amines for CO_2 postcombustion capture applications. *Int. J. Chem. Kinet.* **2018**, *50*, 615−632.

(6) Song, J.-H.; Yoon, J.-H.; Lee, H.; Lee, K.-H. Solubility of Carbon Dioxide in Monoethanolamine + Ethylene Glycol + Water and Monoethanolamine + Poly (ethylene glycol) + Water. *J. Chem. Eng. Data* **1996**, *41*, 497−499.

(7) DuPart, M. S.; Bacon, T. R.; Edwards, D. J. Understanding corrosion in alkanolamine gas treating plants: Part 1. *Hydrocarbon Processing; (United States)* **1993**, *72*, 75−80.

(8) Yang, M. L.; Lv, M.; Chen, J. Efficient non-aqueous solvent formed by 2-piperidineethanol and ethylene glycol for CO_2 absorption. *Chem. Commun.* **2019**, *55*, 12483−12486.

(9) Rochelle, G.; Chen, E.; Freeman, S.; Van Wagener, D.; Xu, Q.; Voice, A. Aqueous piperazine as the new standard for CO_2 capture technology. *Chem. Eng. J.* **2011**, *171*, 725−733.

(10) Chen, X.; Rochelle, G. T. Aqueous piperazine derivatives for CO_2 capture: Accurate screening by a wetted wall column. *Chem. Eng. Res. Des.* **2011**, *89*, 1693−1710.

(11) Heldebrant, D. J.; Koech, P. K.; Glezakou, V.-A.; Rousseau, R.; Malhotra, D.; Cantu, D. C. Water-Lean Solvents for Post-Combustion CO_2 Capture: Fundamentals, Uncertainties, Opportunities, and Outlook. *Chem. Rev.* **2017**, *117*, 9594−9624.

(12) *Accelerating Breakthrough Innovation in Carbon Capture, Utilization, and Storage; Mission Innovation Workshop, September 2017*, U.S. Department of Energy: Houston, Texas, USA, 2017.

(13) Hwang, J.; Kim, J.; Lee, H. W.; Na, J.; Ahn, B. S.; Lee, S. D.; Kim, H. S.; Lee, H.; Lee, U. An experimental based optimization of a novel water lean amine solvent for post combustion CO_2 capture process. *Appl. Energy* **2019**, *248*, 174−184.

(14) Lail, M.; Tanthana, J.; Coleman, L. Non-Aqueous Solvent (NAS) CO2 Capture Process. *Energy Procedia* **2014**, *63*, 580−594.

(15) Bougie, F.; Pokras, D.; Fan, X. Novel non-aqueous MEA solutions for CO2 capture. *Int. J. Greenhouse Gas Control* **2019**, *86*, 34−42.

(16) Nikolic, D.; Wijntje, R.; Patil Hanamant Rao, P.; Van Der Zwet, G. *Sulfinol-X: Second-generation Solvent for Contaminated Gas Treating*, International Petroleum Technology Conference, 2009.

(17) Roberts, B. E.; Mather, A. E. Solubility of H_2S and CO_2 in sulfolane. *The Canadian Journal of Chemical Engineering* **1988**, *66*, 519−520.

(18) Kohl, A. L.; Nielsen, R. B. Alkanolamines for Hydrogen Sulfide and Carbon Dioxide Removal. In *Gas Purification*, 5th ed.; Kohl, A. L.; Nielsen, R. B., Eds.; Gulf Professional Publishing: Houston, 1997; pp. 40−186.

(19) Zou, L.; Gao, H.; Wu, Z.; Liang, Z. Fast screening of amine/physical solvent systems and mass transfer studies on efficient aqueous hybrid MEA/Sulfolane solution for postcombustion CO_2 capture. *J. Chem. Technol. Biotechnol.* **2019**, *95*, 649−664.
(20) Yuan, Y.; Rochelle, G. T. CO_2 absorption rate and capacity of semi-aqueous piperazine for CO_2 capture. *Int. J. Greenhouse Gas Control* **2019**, *85*, 182−186.
(21) Wang, L.; Yu, S.; Li, Q.; Zhang, Y.; An, S.; Zhang, S. Performance of sulfolane/DETA hybrids for CO_2 absorption: Phase splitting behavior, kinetics and thermodynamics. *Appl. Energy* **2018**, *228*, 568−576.
(22) Wang, L.; Zhang, Y.; Wang, R.; Li, Q.; Zhang, S.; Li, M.; Liu, J.; Chen, B. Advanced Monoethanolamine Absorption Using Sulfolane as a Phase Splitter for CO_2 Capture. *Environ. Sci. Technol.* **2018**, *52*, 14556−14563.
(23) Kubisztal, J.; Łosiewicz, B.; Dybal, P.; Kozik, V.; Bak, A. Temperature-Related Corrosion Resistance of AISI 1010 Carbon Steel in Sulfolane. *Materials* **2020**, *13*, 2563−2575.
(24) Carlson, H. G.; E, F. W., Jr. Methanol: Heat Capacity, Enthalpies of Transition and Melting, and Thermodynamic Properties from 5−300°K. *J. Chem. Phys.* **1971**, *54*, 1464−1471.
(25) Pakzad, P.; Mofarahi, M.; Izadpanah, A. A.; Afkhamipour, M. Experimental data, thermodynamic and neural network modeling of CO_2 absorption capacity for 2-amino-2-methyl-1-propanol (AMP) + Methanol (MeOH) + H_2O system. *J. Nat. Gas Sci. Eng.* **2020**, *73*, No. 103060.
(26) Kadiwala, S.; Rayer, A. V.; Henni, A. Kinetics of carbon dioxide (CO_2) with ethylenediamine, 3-amino-1-propanol in methanol and ethanol, and with 1-dimethylamino-2-propanol and 3-dimethylamino-1-propanol in water using stopped-flow technique. *Chem. Eng. J.* **2012**, *179*, 262−271.
(27) Zarker, H. D. Sulfinol—A New Process for Gas Purification. In *6th World Petroleum Congress*, World Petroleum Congress: Frankfurt am Main, Germany, 1963; p. 12.
(28) Rufford, T. E.; Smart, S.; Watson, G. C. Y.; Graham, B. F.; Boxall, J.; Diniz da Costa, J. C.; May, E. F. The removal of CO_2 and N_2 from natural gas: A review of conventional and emerging process technologies. *J. Pet. Sci. Eng.* **2012**, *94-95*, 123−154.
(29) Cieslarova, Z.; dos Santos, V. B.; do Lago, C. L. Both carbamates and monoalkyl carbonates are involved in carbon dioxide capture by alkanolamines. *Int. J. Greenhouse Gas Control* **2018**, *76*, 142−149.
(30) Kim, I.; Jens, C. M.; Grimstvedt, A.; Svendsen, H. F. Thermodynamics of protonation of amines in aqueous solutions at elevated temperatures. *J. Chem. Thermodyn.* **2011**, *43*, 1754−1762.
(31) Zeng, Y.; Chen, X.; Zhao, D.; Li, H.; Zhang, Y.; Xiao, X. Estimation of pKa values for carboxylic acids, alcohols, phenols and amines using changes in the relative Gibbs free energy. *Fluid Phase Equilib.* **2012**, *313*, 148−155.
(32) Kim, J.-H.; Dobrogowska, C.; Hepler, L. G. Thermodynamics of ionization of aqueous alkanolamines. *Can. J. Chem.* **1987**, *65*, 1726−1728.
(33) Weiland, R. H.; Trass, O. Titrimetric determination of acid gases in alkali hydroxides and amines. *Anal. Chem.* **1969**, *41*, 1709−1710.
(34) Idris, Z.; Kummamuru, N. B.; Eimer, D. A. Viscosity measurement of unloaded and CO_2-loaded aqueous monoethanolamine at higher concentrations. *J. Mol. Liq.* **2017**, *243*, 638−645.
(35) Behrendt, W.; Gattow, G.; Dräger, M. Über Chalkogenolate. LXI. Untersuchungen über Halbester der Kohlensäure. 1. Darstellung und Eigenschaften von MonomethyCE und Monoäthylcarbonaten. *Z. Anorg. Allg. Chem.* **1973**, *397*, 237−246.
(36) du Preez, L. J.; Motang, N.; Callanan, L. H.; Burger, A. J. Determining the Liquid Phase Equilibrium Speciation of the CO_2−MEA−H_2O System Using a Simplified in Situ Fourier Transform Infrared Method. *Ind. Eng. Chem. Res.* **2019**, *58*, 469−478.
(37) Sun, C.; Dutta, P. K. Infrared Spectroscopic Study of Reaction of Carbon Dioxide with Aqueous Monoethanolamine Solutions. *Ind. Eng. Chem. Res.* **2016**, *55*, 6276−6283.
(38) Socrates, G., *Infrared and Raman Characteristic Group Frequencies: Tables and Charts*. Wiley: Chichester; New York, 2000.
(39) Richner, G.; Puxty, G. Assessing the Chemical Speciation during CO_2 Absorption by Aqueous Amines Using in Situ FTIR. *Ind. Eng. Chem. Res.* **2012**, *51*, 14317−14324.
(40) Chowdhury, F. A.; Yamada, H.; Higashii, T.; Goto, K.; Onoda, M. CO_2 Capture by Tertiary Amine Absorbents: A Performance Comparison Study. *Ind. Eng. Chem. Res.* **2013**, *52*, 8323−8331.
(41) Schäffer, A.; Brechtel, K.; Scheffknecht, G. Comparative study on differently concentrated aqueous solutions of MEA and TETA for CO_2 capture from flue gases. *Fuel* **2012**, *101*, 148−153.
(42) Barzagli, F.; Lai, S.; Mani, F. Novel non-aqueous amine solvents for reversible CO_2 capture. *Energy Procedia* **2014**, *63*, 1795−1804.
(43) Chen, S.; Chen, S.; Zhang, Y.; Qin, L.; Guo, C.; Chen, J. Species distribution of CO_2 absorption/desorption in aqueous and non-aqueous N-ethylmonoethanolamine solutions. *Int. J. Greenhouse Gas Control* **2016**, *47*, 151−158.
(44) Yamada, H.; Matsuzaki, Y.; Goto, K. Quantitative Spectroscopic Study of Equilibrium in CO_2-Loaded Aqueous 2-(Ethylamino)ethanol Solutions. *Ind. Eng. Chem. Res.* **2014**, *53*, 1617−1623.
(45) Barzagli, F.; Mani, F.; Peruzzini, M. Efficient CO2 absorption and low temperature desorption with non-aqueous solvents based on 2-amino-2-methyl-1-propanol (AMP). *Int. J. Greenhouse Gas Control* **2013**, *16*, 217−223.
(46) Kortunov, P. V.; Siskin, M.; Paccagnini, M.; Thomann, H. CO_2 Reaction Mechanisms with Hindered Alkanolamines: Control and Promotion of Reaction Pathways. *Energy Fuels* **2016**, *30*, 1223−1236.
(47) Rainbolt, J. E.; Koech, P. K.; Yonker, C. R.; Zheng, F.; Main, D.; Weaver, M. L.; Linehan, J. C.; Heldebrant, D. J. Anhydrous tertiary alkanolamines as hybrid chemical and physical CO_2 capture reagents with pressure-swing regeneration. *Energy Environ. Sci.* **2011**, *4*, 480−484.
(48) Heldebrant, D. J.; Koech, P. K.; Rainbolt, J. E.; Zheng, F. CO_2 -binding organic liquids, an integrated acid gas capture system. *Energy Procedia* **2011**, *4*, 216−223.
(49) Kortunov, P. V.; Baugh, L. S.; Siskin, M.; Calabro, D. C. In Situ Nuclear Magnetic Resonance Mechanistic Studies of Carbon Dioxide Reactions with Liquid Amines in Mixed Base Systems: The Interplay of Lewis and Brønsted Basicities. *Energy Fuels* **2015**, *29*, 5967−5989.
(50) Sartori, G.; Savage, D. W. Sterically hindered amines for carbon dioxide removal from gases. *Ind. Eng. Chem. Fundam.* **1983**, *22*, 239−249.
(51) Amundsen, T. G.; Øi, L. E.; Eimer, D. A. Density and Viscosity of Monoethanolamine + Water + Carbon Dioxide from (25 to 80) °C. *J. Chem. Eng. Data* **2009**, *54*, 3096−3100.
(52) Heldebrant, D. J.; Yonker, C. R.; Jessop, P. G.; Phan, L. CO_2 -binding organic liquids (CO_2 BOLs) for post-combustion CO_2 capture. *Energy Procedia* **2009**, *1*, 1187−1195.
(53) Cieslarova, Z.; dos Santos, V. B.; do Lago, C. L. Both carbamates and monoalkyl carbonates are involved in carbon dioxide capyure by alkanolamines. *Int. J. Greenhouse Gas Control* **2018**, *76*, 142−149.

https://doi.org/10.1021/acs.iecr.1c04946
Ind. Eng. Chem. Res. 2022, 61, 5942−5951